DOI: 10.1002/chem.200903580

Phthalocyanine–Polyamine Conjugates as pH-Controlled Photosensitizers for Photodynamic Therapy

Xiong-Jie Jiang,[a] Pui-Chi Lo,[a] Yee-Man Tsang,[b] Sin-Lui Yeung,[b] Wing-Ping Fong,[b] and Dennis K. P. Ng*[a]

Abstract: A series of aryl hydroxyamines prepared by reductive amination were treated with silicon(IV) phthalocyanine dichloride in the presence of pyridine to give the diaxially substituted phthalocyanine–polyamine conjugates **1**–**5**. The electronic absorption, fluorescence emission, and efficiency at generating reactive oxygen species of these compounds were all sensitive to the pH environment. Under acidic conditions, the fluorescence quantum yields and the singlet oxygen quantum yields of these compounds were greatly enhanced in DMF as a result of protonation of the amino moieties, which inhibited the photoinduced electron-transfer deactivation pathway. The Q band was diminished and broadened, and the fluorescence intensity decreased as the pH increased in citrate buffer solutions. The rate of superoxide radical formation was also reduced in a higher pH environment. Compound **3**, containing a terminal 4-chlorophenyl group at the axial substituent, showed the most desirable pH-responsive properties, which makes it a promising tumor-selective fluorescence probe and photosensitizer for photodynamic therapy. All of the phthalocyanines **1**–**5** were highly photocytotoxic against HT29 and HepG2 cells with IC_{50} values as low as 0.03 μM. Compound **3** was highly selective toward lysosomes, but not mitochondria of HT29 cells.

Keywords: photodynamic therapy · photosensitizers · phthalocyanines · polyamines · singlet oxygen

Introduction

Photodynamic therapy (PDT) is a noninvasive therapeutic modality for a variety of premalignant and malignant diseases.[1] It utilizes the combined action of three individually nontoxic components, namely a photosensitizer, light, and molecular oxygen to cause cellular and tissue damage. Singlet oxygen generated through the photosensitization process is believed to be the key cytotoxic reactive oxygen species (ROS) responsible for the damage. As the overall efficacy of the treatment depends greatly on the behavior of the photosensitizers, including their selectivity toward diseased tissues and efficiency at generating ROS, considerable research efforts have been devoted to optimize their photobiological and photophysical characteristics.[2] For targeted delivery of photosensitizers to cancer cells, various approaches have been explored. These include conjugation of photosensitizers to tumor-specific vectors, such as antibodies, synthetic peptides, epidermal growth factor, and adenoviruses,[3] and encapsulation in colloidal carriers, such as liposomes, polymeric micelles, and silica nanoparticles.[4] An alternative strategy takes advantage of the lower extracellular pH in tumors (ca. 6.8) relative to normal tissues (ca. 7.3).[5] The different pH environment may change the stability, aggregation tendency, lipophilicity, and cellular uptake of the photosensitizers, thereby offering a new level of selectivity.

The pH-dependent behavior of several classes of photosensitizers, such as porphyrins,[6] chlorins,[6,7] chalcogenopyrylium dyes,[8] and phenylene vinylenes[9] has been briefly examined. Recently, O'Shea et al. have reported a novel series of amine-containing BF_2-chelated azadipyrromethenes that can switch on and off the singlet-oxygen production in DMF by changing the pH environment.[10] Upon addition of

[a] X.-J. Jiang, Prof. P.-C. Lo, Prof. D. K. P. Ng
Department of Chemistry and Center of Novel Functional Molecules
The Chinese University of Hong Kong
Shatin, N.T. (Hong Kong)
Fax: (+852) 2603-5057
E-mail: dkpn@cuhk.edu.hk

[b] Y.-M. Tsang, S.-L. Yeung, Prof. W.-P. Fong
Department of Biochemistry and Center of Novel Functional Molecules
The Chinese University of Hong Kong
Shatin, N.T. (Hong Kong)

Supporting information for this article is available on the WWW under http://dx.doi.org/10.1002/chem.200903580.

HCl, the singlet oxygen generation rates increase by up to 10-fold. In addition to pH-sensitive photosensitizers, pH-responsive fluorescence probes[11] and polymeric micelles[12] have also received much of current attention because of their potential application in in vitro and in vivo cancer imaging and targeted delivery of chemotherapeutic agents, respectively. All of them work on the basis of the slightly acidic extracellular pH environment of solid tumors.

As part of our continuing efforts in the development of efficient and selective phthalocyanine-based photosensitizers for PDT,[13] we report herein a new series of pH-controlled photosensitizers in which a silicon(IV) phthalocyanine core is axially substituted with aryl polyamine moieties (compounds **1**–**5**). These substituents can modulate the photophysical and photosensitizing properties of the macrocycles in both organic and aqueous media at different pH values. An acid-enhanced fluorescence emission effect has also been observed at the cellular level. These compounds, therefore, serve as potential tumor-selective photosensitizers for PDT. The pH-dependent behavior and the in vitro photodynamic activity of these compounds is reported herein.

Results and Discussion

Scheme 1 shows the synthetic route used to prepare phthalocyanines **1**–**5**. Treatment of hydroxyamines **6**–**7** with benzaldehydes **8**–**11** and $NaBH_4$ led to reductive amination giving compounds **12**–**16** in good yields. The procedure was similar to that reported earlier for the preparation of bis(2-pyridylmethyl)amine.[14] These compounds were then treated with silicon(IV) phthalocyanine dichloride (**17**) in the presence of pyridine in toluene to give the disubstituted products **1**–**5**, which were purified by extraction with CH_2Cl_2 followed by recrystallization from a mixture of $CHCl_3$ and 1-hexane (1:4 v/v). All the new compounds were characterized with various spectroscopic methods and elemental analysis (or accurate mass measurement for hydroxyamines **13**–**16**).

UV/Vis spectra of phthalocyanines **1**–**5** were measured in DMF and the data are summarized in Table 1. The spectra are typical for nonaggregated phthalocyanines, all showing a Soret band at 354 nm, two vibronic bands at 607 and 644 nm, together with a sharp Q band at 674 nm (see the spectra of **1**, Figure S1 in the Supporting Information, given as an example). The absorption positions of all these compounds are identical, which suggests that the axial substituents do not perturb the phthalocyanine π system. Upon excitation at 610 nm, these compounds showed a weak fluorescence emission at 675–677 nm with a fluorescence quantum yield (Φ_F) of 0.01–0.04 relative to unsubstituted zinc(II) phthalocyanine (ZnPc) ($\Phi_F = 0.28$).[15] The weak fluorescence is due to the presence of amino moieties, which quench the singlet excited state of the phthalocyanine core by intramolecular photoinduced electron transfer (PET).[16] Upon addition of HCl (0.6 mM), the emission bands of all the compounds shifted slightly to the red (by 3–5 nm) and increased greatly in intensity (see Figure S2 in the Supporting Information). The fluorescence quantum yield increased significantly to 0.26–0.30 (Table 1). The great changes can be attributed to protonation of the amino moieties under an acidic environment, which inhibits the PET process.[10,11c]

Table 1. Electronic absorption and photophysical data for **1**–**5** in DMF.

Compound	λ_{max} [nm] (log ε)	In the absence of HCl			In the presence of HCl[a]		
		λ_{em}[b]	Φ_F[c]	Φ_Δ[d]	λ_{em}[b]	Φ_F[c]	Φ_Δ[d]
1	354 (4.85), 607 (4.59), 644 (4.52), 674 (5.38)	676	0.04	0.06	681	0.30	0.34
2	354 (4.80), 607 (4.54), 644 (4.47), 674 (5.34)	677	0.01	0.03	680	0.28	0.38
3	354 (4.74), 607 (4.49), 644 (4.43), 674 (5.30)	676	0.01	0.07	681	0.30	0.65
4	354 (4.84), 607 (4.56), 644 (4.49), 674 (5.36)	676	0.01	0.04	681	0.29	0.36
5	354 (4.83), 607 (4.54), 644 (4.49), 674 (5.32)	675	0.02	0.06	680	0.26	0.47

[a] 600 equivalents relative to phthalocyanine. [b] Excited at 610 nm. [c] By using ZnPc in DMF as the reference ($\Phi_F = 0.28$). [d] By using ZnPc as the reference ($\Phi_\Delta = 0.56$ in DMF).

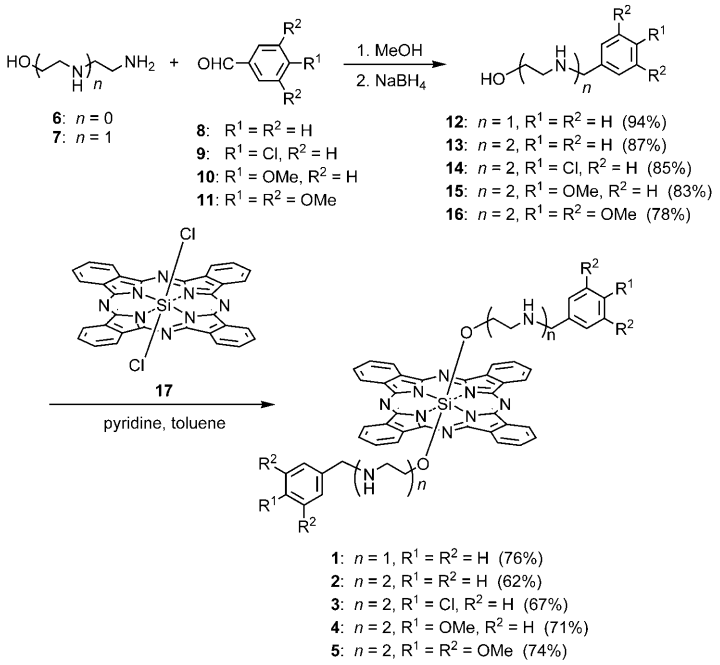

Scheme 1. Preparation of phthalocyanines **1**–**5**.

The absorption and fluorescence spectra of **1**–**5** were also measured in citrate buffer solutions with different pH. Figure 1 shows the UV/Vis spectra of **3** in the buffers given as an example. It can be seen that the Q band remains sharp and intense at pH 4–6. However, it becomes weaker and broadened when the pH increases to 7–8. It is likely that under acidic conditions, the amino moieties are protonated. The charged substituents induce mutual repulsion reducing the aggregation of the phthalocyanine. This results in the occurrence of a sharp and intense monomeric Q band. By contrast, the compound remains aggregated under neutral and

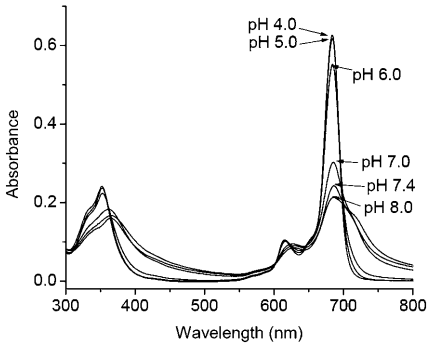

Figure 1. UV/Vis spectra of **3** (3 μM) in citrate buffer solutions with different pH.

slightly alkaline conditions in the buffers leading to a broad and weak Q band.

All of the phthalocyanines **1–5** showed a similar pH-dependent behavior, but the extent was different for different compounds. Figure 2 plots the variation of the Q-band absorbance at 684 nm with the pH value for all these compounds. Generally, the absorbance decreases as the pH increases. Compound **3** shows the most distinct decrease in absorbance when the pH increases from 6.0 to 7.4, which can roughly mimic the environment around tumors and normal tissues, respectively. The change in fluorescence intensity with pH for all these compounds also follows a similar trend as depicted in Figure S3 (Supporting Information). Again, compound **3** shows the most remarkable change and the fluorescence intensity decreases by about 10-fold in the region between pH 6.0 to 7.4. The results show that the axial substituents of **1–5** can modulate the pH-dependent absorption and emission properties of the phthalocyanines in aqueous media, probably through adjustment of the aggregation tendency, and that compound **3** exhibits the most desirable pH-dependent spectral changes.

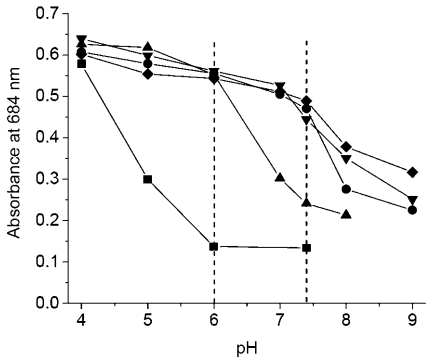

Figure 2. Change in the Q-band absorbance at 684 nm with pH for **1–5** (3 μM) in citrate buffer solutions (■: **1**, ●: **2**, ▲: **3**, ▼: **4**, ◆: **5**).

To evaluate the photosensitizing efficiency of these compounds, their singlet oxygen quantum yields (Φ_Δ) were determined by a steady-state method by using 1,3-diphenylisobenzofuran (DPBF) as the scavenger.[17] The concentration of the quencher was monitored spectroscopically at 414 nm with time (see Figure S4 in the Supporting Information), from which the values of Φ_Δ could be determined. As shown in Table 1, all of the phthalocyanines **1–5** can generate singlet oxygen in DMF, but with a low efficiency. The values of Φ_Δ are only 0.03 to 0.07 relative to ZnPc (Φ_Δ = 0.56).[17] However, in the presence of HCl (600 equiv), their Φ_Δ values are greatly enhanced to 0.34–0.65 and follow the order $\mathbf{1} \approx \mathbf{2} \approx \mathbf{4} < \mathbf{5} < \mathbf{3}$ (Table 1). The significant enhancement can again be attributed to the protonation of the amino moieties, which inhibits the PET process and promotes the intersystem crossing and eventually the singlet oxygen formation.

To better mimic the biological environment, the ROS generation efficiency of phthalocyanines **1–5** was also examined in the buffer solutions by using dihydroethidium (DHE) as a probe for the superoxide radical ($O_2^{\cdot-}$).[18] It is generally believed that ethidium is the oxidized product, which fluoresces strongly at around 600 nm upon excitation. Figure 3 shows the change in fluorescence intensity of ethidium with time when using compound **3** as the sensitizer at two different pH environments (6.0 and 7.4). In the absence of light, no fluorescence could be detected at both pH values, showing that compound **3** could not generate superoxide radicals under these conditions. By contrast, the fluorescence intensity increased steadily upon irradiation and the rate of enhancement was much faster at pH 6.0 relative to that at 7.4. The results show that compound **3** works as an efficient ROS generator, particularly in a low-pH environment. All of the compounds **1–5** exhibit a similar behavior and the results are summarized in Table 2. It can be seen that all of them can generate ROS and are more efficient at pH 6.0 than 7.4. The difference is most remarkable for compound **3**, for which there is a 9.5-fold increase.

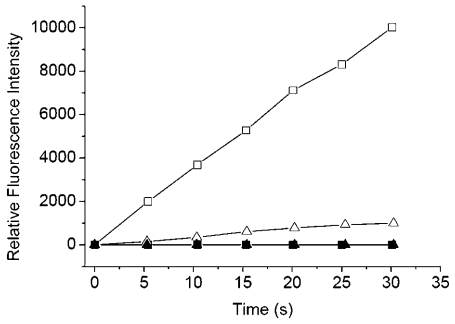

Figure 3. Change in the fluorescence intensity of ethidium with irradiation time (open symbols). The mixture contained phthalocyanine **3** (4 μM) and dihydroethidium (20 μM) in citrate buffer solution at pH 6.0 (■ and □) or 7.4 (▲ and △) and was irradiated with red light ($\lambda >$ 610 nm). The corresponding data obtained without irradiation are given as closed symbols as a control.

The pH-dependent fluorescence emission of **3** at the cellular level was also examined. In this study, human colon adenocarcinoma HT29 cells were incubated with **3** followed with the ionophore nigericin at different pH values (6.0, 6.5,

Table 2. Comparison of the rates of ROS generation by using **1**–**5** as the photosensitizers at pH 6.0 and 7.4.

Compound	Rate of ROS generation (pH 6.0)[a]	Rate of ROS generation (pH 7.4)[a]	Relative rate of ROS generation[b]
1	39	13	3.0
2	345	236	1.5
3	331	35	9.5
4	341	220	1.6
5	238	76	3.1

[a] Determined as the slope of the best-fitted line plotting the fluorescence intensity of ethidium versus irradiation time (as shown in Figure 3). [b] Ratio of the rate of ROS generation at pH 6.0 to that at pH 7.4.

7.4, and 8.0). Nigericin is an H^+/K^+ antiporter, which enables the electroneutral transport of extracellular H^+ ions in exchange for intracellular K^+ ions, and can equilibrate intra- and extracellular pH.[19] The bright field and fluorescence images of the cells were then captured with a confocal microscope (Figure 4a), and the intracellular fluorescence intensities were determined (Figure 4b). As shown in Figure 4, the intracellular intensities are much stronger at pH 6.0 and 6.5 relative to those at pH 7.4 and 8.0. The results further demonstrate that compound **3** is a promising fluorescence probe and photosensitizer that can target tumors on the basis of its remarkable pH-responsive properties in the region between pH 6.5 and 7.4, which are the general pH environments for tumors and normal tissues, respectively.[5]

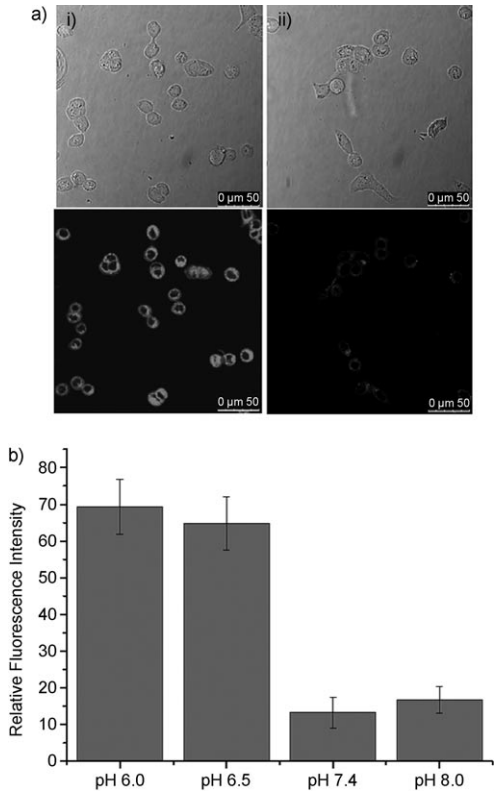

Figure 4. a) Visualization of bright field (upper row) and intracellular fluorescence (lower row) images of HT29 cells after incubation with **3** (0.5 μM) for 30 min, followed by nigericin solutions (25 μM) at i) pH 6.5 and ii) pH 7.4 for 20 min. b) Comparison of the intracellular fluorescence intensity of **3** in the presence of nigericin at different pH values. Data are expressed as the mean ±standard deviation (number of cells = 25).

The photodynamic activities of phthalocyanines **1**–**5** were also evaluated against two different cell lines, namely HT29 and human hepatocarcinoma HepG2 cells. Figure 5 shows

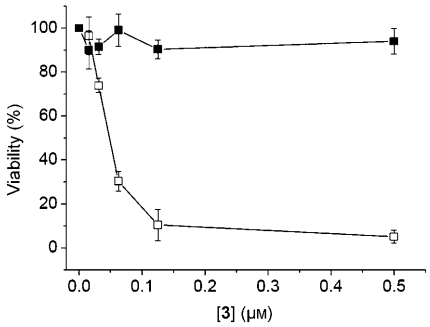

Figure 5. Cytotoxic effects of **3** on HT29 cells in the absence (■) and presence (□) of light ($\lambda > 610$ nm, 40 mW cm^{-2}, 48 J cm^{-2}). Data are expressed as the mean ±standard error of the means of three independent experiments, each performed in quadruplicate.

the effects of **3** on HT29 cells, which are typical for all these phthalocyanines. All of them are essentially noncytotoxic in the absence of light, but exhibit high photocytotoxicity. The IC_{50} values, defined as the dye concentration required to kill 50% of the cells, are summarized in Table 3. Compounds **2**–**5** are highly potent with IC_{50} values in the range of 0.03 to 0.06 μM, which are comparable with those of some other silicon(IV) phthalocyanine-based photosensitizers reported by us earlier.[13a,16,20] Compound **1**, which only has one amino group in the axial substituent is significantly less photocytotoxic. This can easily be seen in Figure S5 (Supporting Information), which compares the effects of **1** and **2** on HepG2 cells. The IC_{50} values of **1** (0.45–0.49) are roughly 10-fold higher relative to those of the other analogues (Table 3).

Table 3. Comparison of the IC_{50} values of phthalocyanines **1**–**5** against HT29 and HepG2 cells.

Compound	IC_{50} [μM]	
	HT29	HepG2
1	0.45	0.49
2	0.03	0.06
3	0.05	0.06
4	0.03	0.03
5	0.03	0.06

The subcellular localization of **3** in HT29 cells was also investigated. The cells were stained with **3** together with LysoTracker Green DND 26 or MitoTracker Green FM, which are specific fluorescence dyes for lysosomes and mitochondria, respectively. As shown in Figure 6a–c, the fluorescence

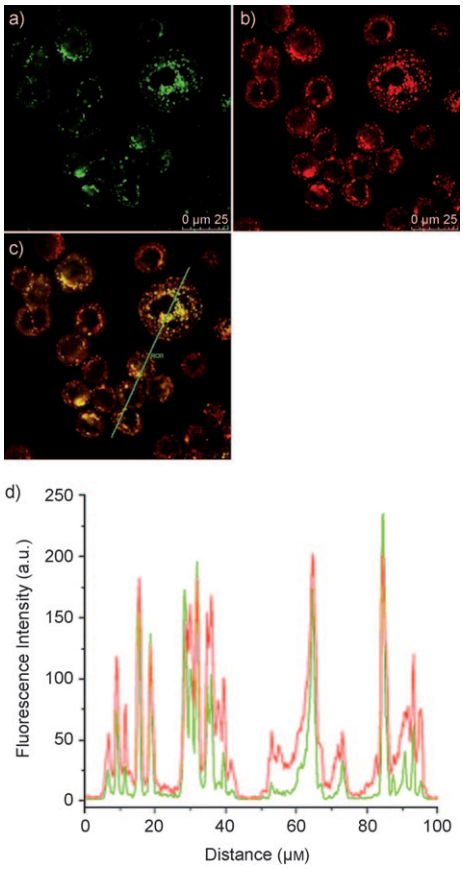

Figure 6. Visualization of the intracellular fluorescence of HT29 by using filter sets specific for a) phthalocyanine **3** (in green) and b) LysoTracker (in red), and c) the corresponding superimposed image. Figure (d) shows the fluorescence intensity profiles of **3** (green) and LysoTracker (red) traced along the line in (d).

caused by the LysoTracker (excited at 488 nm, monitored at 500–570 nm) is well superimposed with the fluorescence caused by **3** (excited at 633 nm, monitored at 640–700 nm). The very similar fluorescence intensity profiles of **3** and LysoTracker traced along the green line in Figure 6c (Figure 6d) also confirms that compound **3** can target the lysosomes of the cells. By contrast, the fluorescence images of **3** and the Mitotracker (excited at 488 nm, monitored at 500–570 nm) cannot be superimposed (see Figure S6 in the Supporting Information), which indicates that **3** is not localized in the mitochondria.

Conclusion

In summary, we have prepared and characterized a series of novel silicon(IV) phthalocyanines axially substituted with aryl polyamine moieties. These compounds show pH-dependent UV/Vis and fluorescence spectroscopic properties in DMF and citrate buffer solutions. In acidic media, all of them can generate ROS including singlet oxygen and the superoxide radical effectively as a result of protonation of the amino moieties that inhibit the PET process. Compound **3** is of particular interest because of its remarkably different behavior in the pH range (ca. 6.5 to 7.4) differentiating the tumor and normal tissue environments. Phthalocyanines **1**–**5** also exhibit high photocytotoxicity against HT29 and HepG2 cells with IC_{50} values as low as 0.03 µM. As revealed by confocal microscopy, compound **3** also shows a high selectivity towards the lysosomes of the cells. The results presented herein show that these phthalocyanines, particularly compound **3**, are promising pH-controlled and tumor-selective photosensitizers for PDT.

Experimental Section

Materials and methods: All the reactions were performed under an atmosphere of nitrogen. THF, DMF, pyridine, and toluene were distilled from sodium benzophenone ketyl, barium oxide, calcium hydride, and sodium, respectively. All other solvents and reagents were of reagent grade and used as received.

^{1}H and ^{13}C{^{1}H} NMR spectra were recorded on a Bruker DPX 300 spectrometer (^{1}H, 300; ^{13}C, 75.4 MHz) in $CDCl_3$. Spectra were referenced internally by using the residual solvent (^{1}H: $\delta = 7.26$ ppm) or solvent (^{13}C: $\delta = 77.0$ ppm) resonances relative to $SiMe_4$. Fast-atom bombardment (FAB) and electrospray ionization (ESI) mass spectra were recorded on a Thermo Finnigan MAT 95 XL mass spectrometer. Elemental analyses were performed by the Shanghai Institute of Organic Chemistry, Chinese Academy of Sciences.

UV/Vis and steady-state fluorescence spectra were taken on a Cary 5G UV/Vis-NIR spectrophotometer and a Hitachi F-7000 spectrofluorometer, respectively. The Φ_F values were determined by the equation: $\Phi_{F(sample)} = (F_{sample}/F_{ref})(A_{ref}/A_{sample})(n^2_{sample}/n^2_{ref})\Phi_{F(ref)}$,[21] in which F, A, and n are the measured fluorescence (area under the emission peak), the absorbance at the excitation position (610 nm), and the refractive index of the solvent, respectively. ZnPc in DMF was used as the reference ($\Phi_{F(ref)} = 0.28$).[15] To minimize reabsorption of radiation by the ground-state species, the emission spectra were obtained in very dilute solutions of which the absorbance at 610 nm was about 0.03. The Φ_Δ values were measured in DMF by the method of chemical quenching of DPBF by using ZnPc as a reference ($\Phi_\Delta = 0.56$).[17]

ROS measurements for **1**–**5** were performed in citrate buffer solutions with pH values at 6.0 and 7.4. A mixture of the phthalocyanine (4 µM) and dihydroethidium (20 µM) in the buffer (3 mL, at pH 6.0 or 7.4) was prepared in a quartz cell. Its fluorescence spectra ($\lambda_{ex} = 465$ nm, $\lambda_{em} =$ 500–700 nm due to the oxidized product) were recorded immediately after irradiation with a red light for every 5 s. The light source consisted of a 100 W halogen lamp and a color glass filter (Newport) cut-on 610 nm. The rate of oxidation of dihydroethidium, which reflects the ROS generation efficiency of that phthalocyanine, was monitored for a total of 30 s irradiation.

Hydroxyamine 12: A solution of benzaldehyde (**8**) (2.80 g, 26.4 mmol) in methanol (150 mL) was cooled in an ice bath. 2-Aminoethanol (**6**) (1.40 g, 22.9 mmol) was then added, and the mixture was stirred at room temperature for 8 h. Sodium borohydride (2.00 g, 52.9 mmol) was added slowly to the reaction mixture, which was maintained at 0 °C by using an ice bath. After the addition, the mixture was stirred at room temperature for 12 h. The reaction was quenched by the addition of HCl (6 M) with cooling until the pH was adjusted to 4. The solvent was removed under reduced pressure. The residue was dissolved in water (100 mL) and washed with CH_2Cl_2 (100 mL × 3) to remove the organic impurities. The aqueous phase was separated and its pH was adjusted to 10 by using solid Na_2CO_3. It was then extracted with CH_2Cl_2 (150 mL). The organic portion was dried over anhydrous $MgSO_4$ and evaporated in vacuo to give the product as a colorless oil (3.25 g, 94 %). ^{1}H NMR: $\delta = 7.27$–7.33 (m, 5H; ArH), 3.80 (s, 2H; CH_2), 3.65 (t, $J = 5.1$ Hz, 2H; CH_2), 2.80 ppm (t, $J = 5.1$ Hz, 2H; CH_2); ^{13}C{^{1}H} NMR: $\delta = 138.9$, 128.1, 128.0, 126.8,

60.0, 53.0, 50.3 ppm; the NMR spectroscopic data are essentially the same as those given elsewhere.[22]

Hydroxyamine 13: According to the procedure described for **12**, compound **13** was prepared as a colorless oil by treating benzaldehyde (**8**) (2.12 g, 20.0 mmol) with 2-(2-aminoethylamino)ethanol (**7**) (2.08 g, 20.0 mmol), followed by reduction with sodium borohydride (1.52 g, 40.2 mmol) (3.38 g, 87%). ^{1}H NMR: δ = 7.27–7.33 (m, 5H; ArH), 3.78 (s, 2H; CH_2), 3.62 (t, J = 5.1 Hz, 2H; CH_2), 2.71–2.74 ppm (m, 6H; CH_2); ^{13}C{^{1}H} NMR: δ = 139.9, 128.2, 128.0, 126.8, 60.4, 53.7, 51.2, 48.7, 48.4 ppm; MS (FAB): m/z (%): 195 $[M+H]^+$ (100); HRMS (FAB): m/z: calcd for $C_{11}H_{19}N_2O$: 195.1492 $[M+H]^+$; found: 195.1490.

Hydroxyamine 14: According to the procedure described for **12**, compound **14** was synthesized by treating 4-chlorobenzaldehyde (**9**) (1.97 g, 14.0 mmol) with 2-(2-aminoethylamino)ethanol (**7**) (1.46 g, 14.0 mmol), followed by reduction with sodium borohydride (1.06 g, 28.0 mmol). The product was isolated as a brown oil (2.72 g, 85%). ^{1}H NMR: δ = 7.22–7.29 (m, 4H; ArH), 3.73 (s, 2H; CH_2), 3.61 (t, J = 5.4 Hz, 2H; CH_2), 2.69–2.72 ppm (m, 6H; CH_2); ^{13}C{^{1}H} NMR: δ = 138.5, 132.5, 129.4, 128.4, 60.6, 53.0, 51.2, 48.7, 48.5 ppm; MS (FAB): m/z (%): 229 $[M]^+$ (100); HRMS (FAB): m/z: calcd for $C_{11}H_{17}ClN_2O$: 229.1102 $[M]^+$; found: 229.1094.

Hydroxyamine 15: According to the procedure described for **12**, 4-methoxybenzaldehyde (**10**) (1.91 g, 14.0 mmol) was treated with 2-(2-aminoethylamino)ethanol (**7**) (1.46 g, 14.0 mmol) and sodium borohydride (1.06 g, 28.0 mmol) to give **15** as a brown oil (2.61 g, 83%). ^{1}H NMR: δ = 7.24 (d, J = 8.7 Hz, 2H; ArH), 6.87 (d, J = 8.7 Hz, 2H; ArH), 3.80 (s, 3H; CH_3), 3.74 (s, 2H; CH_2), 3.64 (t, J = 5.4 Hz, 2H; CH_2), 2.75–2.79 ppm (m, 6H; CH_2); ^{13}C{^{1}H} NMR: δ = 158.7, 131.7, 129.5, 113.8, 60.5, 55.2, 53.1, 51.0, 48.4, 48.1 ppm; MS (FAB): m/z (%): 121 $[C_6H_4(OCH_3)CH_2]^+$ (100), 225 $[M+H]^+$ (54); HRMS (FAB): m/z: calcd for $C_{12}H_{21}N_2O_2$: 225.1598 $[M+H]^+$; found: 225.1605.

Hydroxyamine 16: According to the procedure described for **12**, 3,4,5-trimethoxybenzaldehyde (**11**) (2.75 g, 14.0 mmol) was reacted with 2-(2-aminoethylamino)ethanol (**7**) (1.46 g, 14.0 mmol) and sodium borohydride (1.06 g, 28.0 mmol) to give **16** as a brown oil (3.11 g, 78%). ^{1}H NMR: δ = 6.56 (s, 2H; ArH), 3.87 (s, 6H; CH_3), 3.83 (s, 3H; CH_3), 3.74 (s, 2H; CH_2), 3.64 (t, J = 5.1 Hz, 2H; CH_2), 2.75–2.78 ppm (m, 6H; CH_2); ^{13}C{^{1}H} NMR: δ = 153.2, 136.8, 135.6, 104.9, 60.8, 60.7, 56.1, 54.1, 51.0, 48.5, 48.4 ppm; MS (FAB): m/z (%): 181 $[C_6H_2(OCH_3)_3CH_2]^+$ (100), 285 $[M+H]^+$ (13); HRMS (FAB): m/z: calcd for $C_{14}H_{25}N_2O_4$: 285.1809 $[M+H]^+$; found: 285.1806.

Phthalocyanine 1: A mixture of silicon(IV) phthalocyanine dichloride (**17**) (0.20 g, 0.33 mmol), 2-benzylaminoethanol (**12**) (0.15 g, 1.0 mmol), and pyridine (0.5 mL) in toluene (30 mL) was refluxed for 4 h. After evaporating the solvent in vacuo, the residue was dissolved in CH_2Cl_2 (100 mL) and then washed with water (100 mL × 3). The organic layer was collected and evaporated under reduced pressure. The crude product was recrystallized from $CHCl_3$/1-hexane (1:4 v/v) to give the product as a blue solid (0.21 g, 76%). ^{1}H NMR: δ = 9.60–9.64 (m, 8H; Pc-H$_\alpha$), 8.32–8.36 (m, 8H; Pc-H$_\beta$), 6.94 (t, J = 7.2 Hz, 2H; ArH), 6.84 (t, J = 7.2 Hz, 4H; ArH), 6.09 (d, J = 7.2 Hz, 4H; ArH), 2.01 (s, 4H; CH_2), −0.27 (t, J = 5.4 Hz, 4H; CH_2), −1.93 ppm (t, J = 5.4 Hz, 4H; CH_2); ^{13}C{^{1}H} NMR: δ = 149.2, 139.5, 135.9, 130.9, 127.7, 126.9, 126.0, 123.7, 53.7, 51.3, 47.6 ppm; HRMS (ESI): m/z: calcd for $C_{50}H_{40}N_{10}NaO_2Si$: 863.2997 $[M+Na]^+$; found: 863.2999; elemental analysis calcd (%) for $C_{50}H_{40}N_{10}O_2Si$: C 71.41, H 4.79, N 16.65; found: C 71.56, H 5.06, N 16.36.

Phthalocyanine 2: According to the procedure described for **1**, silicon(IV) phthalocyanine dichloride (**17**) (0.20 g, 0.33 mmol) was treated with hydroxyamine **13** (0.19 g, 1.0 mmol) and pyridine (0.5 mL) in toluene (30 mL) to give **2** as a blue solid (0.19 g, 62%). ^{1}H NMR: δ = 9.58–9.62 (m, 8H; Pc-H$_\alpha$), 8.29–8.33 (m, 8H; Pc-H$_\beta$), 7.20–7.25 (m, 6H; ArH), 7.00 (d, J = 7.5 Hz, 4H; ArH), 3.26 (s, 4H; CH_2), 1.58 (t, J = 6.0 Hz, 4H; CH_2), 0.88 (t, J = 6.0 Hz, 4H; CH_2), −0.35 (t, J = 5.4 Hz, 4H; CH_2), −1.97 ppm (t, J = 5.4 Hz, 4H; CH_2); ^{13}C{^{1}H} NMR: δ = 149.2, 140.3, 135.9, 131.0, 128.1, 127.9, 126.6, 123.6, 53.7, 53.3, 47.8 (two overlapping signals), 46.9 ppm; HRMS (ESI): m/z: calcd for $C_{54}H_{51}N_{12}O_2Si$: 927.4022 $[M+H]^+$; found: 927.4029; elemental analysis calcd (%) for $C_{54}H_{52}N_{12}O_3Si$ (**2**·H_2O): C 68.62, H 5.55, N 17.78; found: C 68.45, H 5.79, N 17.33.

Phthalocyanine 3: According to the procedure described for **1**, silicon(IV) phthalocyanine dichloride (**17**) (0.20 g, 0.33 mmol) was treated with hydroxyamine **14** (0.23 g, 1.0 mmol) and pyridine (0.5 mL) in toluene (30 mL) to give **3** as a blue solid (0.22 g, 67%). ^{1}H NMR: δ = 9.57–9.61 (m, 8H; Pc-H$_\alpha$), 8.30–8.34 (m, 8H; Pc-H$_\beta$), 7.19 (d, J = 8.4 Hz, 4H; ArH), 6.89 (d, J = 8.4 Hz, 4H; ArH), 3.21 (s, 4H; CH_2), 1.55 (t, J = 5.7 Hz, 4H; CH_2), 0.89 (t, J = 5.7 Hz, 4H; CH_2), −0.34 (t, J = 5.1 Hz, 4H; CH_2), −1.97 ppm (t, J = 5.1 Hz, 4H; CH_2); ^{13}C{^{1}H} NMR: δ = 149.2, 138.9, 135.9, 132.2, 131.0, 129.1, 128.2, 123.6, 53.8, 52.5, 47.9, 47.7, 46.9 ppm; HRMS (FAB): m/z: calcd for $C_{54}H_{49}Cl_2N_{12}O_2Si$: 995.3242 $[M+H]^+$; found: 995.3214; elemental analysis calcd (%) for $C_{54}H_{48}Cl_2N_{12}O_2Si$: C 65.12, H 4.86, N 16.87; found: C 64.75, H 4.62, N 16.56.

Phthalocyanine 4: According to the procedure described for **1**, silicon(IV) phthalocyanine dichloride (**17**) (0.20 g, 0.33 mmol) was treated with hydroxyamine **15** (0.22 g, 1.0 mmol) and pyridine (0.5 mL) in toluene (30 mL) to give **4** as a blue solid (0.23 g, 71%). ^{1}H NMR: δ = 9.59–9.62 (m, 8H; Pc-H$_\alpha$), 8.30–8.33 (m, 8H; Pc-H$_\beta$), 6.91 (d, J = 8.4 Hz, 4H; ArH), 6.76 (d, J = 8.4 Hz, 4H; ArH), 3.78 (s, 6H; CH_3), 3.19 (s, 4H; CH_2), 1.56 (t, J = 6.0 Hz, 4H; CH_2), 0.88 (t, J = 6.0 Hz, 4H; CH_2), −0.36 (t, J = 5.4 Hz, 4H; CH_2), −1.98 ppm (t, J = 5.4 Hz, 4H; CH_2); ^{13}C{^{1}H} NMR: δ = 158.3, 149.2, 135.9, 132.5, 130.9, 129.0, 123.7, 113.5, 55.2, 53.8, 52.7, 47.9, 47.7, 46.9 ppm; HRMS (FAB): m/z: calcd for $C_{56}H_{55}N_{12}O_4Si$: 987.4233 $[M+H]^+$; found: 987.4196; elemental analysis calcd (%) for $C_{56}H_{56}N_{12}O_5Si$ (**4**·H_2O): C 66.91, H 5.62, N 16.72; found: C 67.36, H 5.53, N 16.45.

Phthalocyanine 5: According to the procedure described for **1**, silicon(IV) phthalocyanine dichloride (**17**) (0.20 g, 0.33 mmol) was treated with hydroxyamine **16** (0.28 g, 1.0 mmol) and pyridine (0.5 mL) in toluene (30 mL) to give **5** as a blue solid (0.27 g, 74%). ^{1}H NMR: δ = 9.59–9.62 (m, 8H; Pc-H$_\alpha$), 8.31–8.34 (m, 8H; Pc-H$_\beta$), 6.20 (s, 4H; ArH), 3.78 (s, 6H; CH_3), 3.72 (s, 12H; CH_3), 3.19 (s, 4H; CH_2), 1.59 (t, J = 6.0 Hz, 4H; CH_2), 0.91 (t, J = 6.0 Hz, 4H; CH_2), −0.34 (t, J = 5.1 Hz, 4H; CH_2), −1.96 ppm (t, J = 5.1 Hz, 4H; CH_2); ^{13}C{^{1}H} NMR: δ = 152.9, 149.2, 136.5, 136.1, 135.9, 131.0, 123.6, 104.5, 60.8, 55.9, 53.7, 53.5, 47.9, 47.7, 46.9 ppm; HRMS (FAB): m/z: calcd for $C_{60}H_{63}N_{12}O_8Si$: 1107.4656 $[M+H]^+$; found: 1107.4604; elemental analysis calcd (%) for $C_{60}H_{64}N_{12}O_9Si$: (**5**·H_2O): C 64.04, H 5.73, N 14.94; found: C 64.21, H 5.91, N 14.79.

Cell lines and culture conditions: The HT29 human colorectal carcinoma cells (from ATCC, no. HTB-38) were maintained in Dulbecco's modified Eagle's medium (DMEM; Invitrogen, no.10313–021) supplemented with fetal calf serum (10%), penicillin-streptomycin (100 units ml^{-1} and 100 μg mL^{-1}, respectively), L-glutamine (2 mM), and transferrin (10 μg mL^{-1}). The HepG2 human hepatocarcinoma cells (from ATCC, no. HB-8065) were maintained in RPMI medium 1640 (Invitrogen, no. 23400–021) supplemented with fetal calf serum (10%) and penicillin-streptomycin (100 units ml^{-1} and 100 μg mL^{-1}, respectively). Approximately 3×10^4 (for HT29) or 4×10^4 (for HepG2) cells per well in these media were inoculated in 96-multiwell plates and incubated overnight at 37 °C in a humidified 5% CO_2 atmosphere.

pH-dependent intracellular fluorescence studies: About 1.2×10^5 HT29 cells in the growth medium (2 mL) were seeded on a coverslip and incubated overnight at 37 °C under 5% CO_2. The medium was removed, then the cells were incubated with a solution of phthalocyanine **3** in the medium (0.5 μM, 2 mL) for 30 min under the same conditions. The cells were then rinsed with phosphate buffered saline (PBS) and incubated with nigericin (Sigma) in PBS (25 μM, 2 mL) at different pH values (6.0, 6.5, 7.4, and 8.0) for a further 20 min. The cells were viewed with a Leica SP5 confocal microscope equipped with a 633 nm helium neon laser. Emission signals from 640–700 nm (gain = 750 V) were collected and the images were digitized and analyzed by Leica Application Suite Advanced Fluorescence. The intracellular fluorescence intensities (total 25 cells for each pH solution) were also determined.

Photocytotoxicity assay: Phthalocyanines **1–5** were first dissolved in THF to give 1.6 mM solutions, which were diluted to appropriate concentra-

tions with the culture medium. The cells, after being rinsed with PBS, were incubated with 100 μL of these phthalocyanine solutions for 2 h at 37 °C under 5 % CO_2. The cells were then rinsed again with PBS and refilled with 100 μL of the culture medium before being illuminated at ambient temperature. The light source consisted of a 300 W halogen lamp, a water tank for cooling, and a color glass filter (Newport) cut-on 610 nm. The fluence rate ($\lambda > 610$ nm) was 40 mW cm^{-2}. An illumination of 20 min led to a total fluence of 48 J cm^{-2}.

Cell viability was determined by means of the colorimetric MTT assay.[23] After illumination, the cells were incubated at 37 °C under 5 % CO_2 overnight. An MTT (Sigma) solution in PBS (3 mg mL^{-1}, 50 μL) was added to each well followed by incubation for 2 h under the same environment. A solution of sodium dodecyl sulfate (SDS, Sigma; 10 % by weight, 50 μL) was then added to each well. The plate was incubated in an oven at 60 °C for 30 min, then 80 μL of *iso*-propanol was added to each well. The plate was agitated on a Bio-Rad microplate reader at ambient temperature for 10 s before the absorbance at 540 nm at each well was taken. The average absorbance of the blank wells, which did not contain the cells, was subtracted from the readings of the other wells. The cell viability was then determined by the following equation: % viability $= [\Sigma(A_i/A_{control} \times 100)]/n$, in which A_i is the absorbance of the ith data ($i = 1, 2, .., n$), $A_{control}$ is the average absorbance of the control wells in which the phthalocyanine was absent, and n (=4) is the number of data points.

Subcellular localization studies: About 6.0×10^4 HT29 cells in the culture medium (2 mL) were seeded on a coverslip and incubated overnight at 37 °C under 5 % CO_2. The medium was then removed. For the study with LysoTracker, the cells were incubated with a solution of **3** in the medium (0.5 μM, 2 mL) for 115 min under the same conditions. LysoTracker Green DND 26 (Molecular Probes; 2 μM in the culture medium) was then added, and the cells were incubated under these conditions for a further 5 min. For the study with MitoTracker, the cells were incubated with MitoTracker Green FM (Molecular Probes; 0.2 μM) in the medium (2 mL) for 30 min. Then the cells were rinsed with PBS and incubated again with a solution of **3** in the medium (2 μM, 2 mL) for 2 h under the same conditions. For both cases, the cells were then rinsed with PBS and viewed with a Leica SP5 confocal microscope equipped with a 488 nm Argon laser and a 633 helium neon laser. Both LysoTracker and MitroTracker were excited at 488 nm and monitored at 500–570 nm, whereas compound **3** was excited at 633 nm and monitored at 640–700 nm. Images were digitized and analyzed by using Leica Application Suite Advanced Fluorescence. The subcellular localization of **3** was revealed by comparing the intracellular fluorescence images caused by the LysoTracker or MitoTracker and this dye.

Acknowledgements

This work was supported by a grant from the Research Grants Council of the Hong Kong Special Administrative Region, China (project no. 402608) and a strategic investments scheme administered by The Chinese University of Hong Kong.

[1] a) D. E. J. G. J. Dolmans, D. Fukumura, R. K. Jain, *Nat. Rev. Cancer* **2003**, *3*, 380–387; b) S. B. Brown, E. A. Brown, I. Walker, *Lancet Oncol.* **2004**, *5*, 497–508; c) B. C. Wilson, M. S. Patterson, *Phys. Med. Biol.* **2008**, *53*, R61–R109.

[2] a) M. R. Detty, S. L. Gibson. S. J. Wagner, *J. Med. Chem.* **2004**, *47*, 3897–3915; b) E. S. Nyman, P. H. Hynninen, *J. Photochem. Photobiol. B* **2004**, *73*, 1–28.

[3] a) W. M. Sharman, J. E. van Lier, C. M. Allen, *Adv. Drug Delivery Rev.* **2004**, *56*, 53–76; b) N. Solban, I. Rizvi, T. Hasan, *Lasers Surg. Med.* **2006**, *38*, 522–531; c) S. Verma, G. M. Watt, Z. Mai, T. Hasan, *Photochem. Photobiol.* **2007**, *83*, 996–1005.

[4] a) I. Roy, T. Y. Ohulchanskyy, H. E. Pudavar, E. J. Bergey, A. R. Oseroff, J. Morgan, T. J. Dougherty, P. N. Prasad, *J. Am. Chem. Soc.* **2003**, *125*, 7860–7865; b) N. Nishiyama, W.-D. Jang, K. Kataoka, *New J. Chem.* **2007**, *31*, 1074–1082; c) L. Zhang, F. X. Gu, J. M. Chan, A. Z. Wang, R. S. Langer, O. C. Farokhzad, *Clin. Pharmacol. Ther.* **2008**, *83*, 761–769.

[5] a) L. E. Gerweck, K. Seetharaman, *Cancer Res.* **1996**, *56*, 1194–1198; b) M. Stubbs, P. M. J. McSheehy, J. R. Griffiths, C. L. Bashford, *Mol. Med. Today* **2000**, *6*, 15–19; c) L. E. Gerweck, *Drug Resist. Updates* **2000**, *3*, 49–50.

[6] a) J. Moan, L. Smedshammer, T. Christensen, *Cancer Lett.* **1980**, *9*, 327–332; b) B. Cunderlíková, E. G. Bjørklund, E. O. Pettersen, J. Moan, *Photochem. Photobiol.* **2001**, *74*, 246–252; c) E. G. Friberg, B. Cunderlíková, E. O. Pettersen, J. Moan, *Cancer Lett.* **2003**, *195*, 73–80; d) B. Cunderlíková, J. Moan, I. Sjaastad, *Cancer Lett.* **2005**, *222*, 39–47.

[7] a) B. Cunderlíková, L. Gangeskar, J. Moan, *J. Photochem. Photobiol. B* **1999**, *53*, 81–90; b) M. Sharma, A. Dube, H. Bansal, P. K. Gupta, *Photochem. Photobiol. Sci.* **2004**, *3*, 231–235; c) M. Sharma, K. Sahu, A. Dube, P. K. Gupta, *J. Photochem. Photobiol. B* **2005**, *81*, 107–113; d) H. Mojzisova, S. Bonneau, C. Vever-Bizet, D. Brault, *Biochim. Biophys. Acta Biomembr.* **2007**, *1768*, 2748–2756.

[8] D. A. Bellnier, D. N. Young, M. R. Detty, S. H. Camacho, A. R. Oseroff, *Photochem. Photobiol.* **1999**, *70*, 630–636.

[9] J. Arnbjerg, M. Johnsen, C. B. Nielsen, M. Jørgensen, P. R. Ogilby, *J. Phys. Chem. A* **2007**, *111*, 4573–4583.

[10] S. O. McDonnell, M. J. Hall, L. T. Allen, A. Byrne, W. M. Gallagher, D. F. O'Shea, *J. Am. Chem. Soc.* **2005**, *127*, 16360–16361.

[11] For some recent examples, see: a) S. A. Hilderbrand, K. A. Kelly, M. Niedre, R. Weissleder, *Bioconjugate Chem.* **2008**, *19*, 1635–1639; b) B. Tang, F. Yu, P. Li, L. Tong, X. Duan, T. Xie, X. Wang, *J. Am. Chem. Soc.* **2009**, *131*, 3016–3023; c) Y. Urano, D. Asanuma, Y. Hama, Y. Koyama, T. Barrett, M. Kamiya, T. Nagano, T. Watanabe, A. Hasegawa, P. L. Choyke, H. Kobayashi, *Nat. Med.* **2009**, *15*, 104–109.

[12] E. S. Lee, Z. Gao, Y. H. Bae, *J. Controlled Release* **2008**, *132*, 164–170.

[13] See, for example: a) P.-C. Lo, C. M. H. Chan, J.-Y. Liu, W.-P. Fong, D. K. P. Ng, *J. Med. Chem.* **2007**, *50*, 2100–2107; b) S. C. H. Leung, P.-C. Lo, D. K. P. Ng, W.-K. Liu, K.-P. Fung, W.-P. Fong, *Br. J. Pharmacol.* **2008**, *154*, 4–12; c) J.-Y. Liu, X.-J. Jiang, W.-P. Fong, D. K. P. Ng, *Org. Biomol. Chem.* **2008**, *6*, 4560–4566; d) J.-Y. Liu, P.-C. Lo, X.-J. Jiang, W.-P. Fong, D. K. P. Ng, *Dalton Trans.* **2009**, 4129–4135.

[14] N. M. F. Carvalho, A. Horn, Jr., A. J. Bortoluzzi, V. Drago, O. A. C. Antunes, *Inorg. Chim. Acta* **2006**, *359*, 90–98.

[15] I. Scalise, E. N. Durantini, *Bioorg. Med. Chem.* **2005**, *13*, 3037–3045.

[16] P.-C. Lo, J.-D. Huang, D. Y. Y. Cheng, E. Y. M. Chan, W.-P. Fong, W.-H. Ko, D. K. P. Ng, *Chem. Eur. J.* **2004**, *10*, 4831–4838.

[17] M. D. Maree, N. Kuznetsova, T. Nyokong, *J. Photochem. Photobiol. A* **2001**, *140*, 117–125.

[18] a) H. Zhao, S. Kalivendi, H. Zhang, J. Joseph, K. Nithipatikom, J. Vásquez-Vivar, B. Kalyanaraman, *Free Radical Biol. Med.* **2003**, *34*, 1359–1368; b) B. Halliwell, M. Whiteman, *Br. J. Pharmacol.* **2004**, *142*, 231–255.

[19] a) E. Jähde, K.-H. Glüsenkamp, M. F. Rajewsky, *Cancer Chemother. Pharmacol.* **1991**, *27*, 440–444; b) M. E. Varnes, M. T. Bayne, G. R. Bright, *Photochem. Photobiol.* **1996**, *64*, 853–858.

[20] a) P. P. S. Lee, P.-C. Lo, E. Y. M. Chan, W.-P. Fong, W.-H. Ko, D. K. P. Ng, *Tetrahedron Lett.* **2005**, *46*, 1551–1554; b) X. Leng, C.-F. Choi, P.-C. Lo, D. K. P. Ng, *Org. Lett.* **2007**, *9*, 231–234; c) P.-C. Lo, S. C. H. Leung, E. Y. M. Chan, W.-P. Fong, W.-H. Ko, D. K. P. Ng, *Photodiagn. Photodyn. Ther.* **2007**, *4*, 117–123; d) P.-C. Lo, W.-P. Fong, D. K. P. Ng, *ChemMedChem* **2008**, *3*, 1110–1117.

[21] D. F. Eaton, *Pure Appl. Chem.* **1988**, *60*, 1107–1114.

[22] *The Aldrich Library of ^{13}C and ^{1}H FT NMR Spectra, Vol. 2* (Eds.: C. J. Pouchert, J. Behnke), Aldrich Chemical Company, Milwaukee, **1993**.

[23] H. Tada, O. Shiho, K. Kuroshima, M. Koyama, K. Tsukamoto, *J. Immunol. Methods* **1986**, *93*, 157–165.

Received: December 30, 2009
Published online: March 22, 2010

